ФИЗИКА ЭЛЕМЕНТАРНЫХ ЧАСТИЦ И АТОМНОГО ЯДРА
2008. Т. 39. ВЫП. 2

THE COMPRESSION MODES IN ATOMIC NUCLEI AND THEIR RELEVANCE FOR THE NUCLEAR EQUATION OF STATE

G. Colò

Dipartimento di Fisica, Università degli Studi, and INFN, Sezione di Milano, Milano, Italy

ФИЗИКА ЭЛЕМЕНТАРНЫХ ЧАСТИЦ И АТОМНОГО ЯДРА
2008. Т. 39. ВЫП. 2

THE COMPRESSION MODES IN ATOMIC NUCLEI AND THEIR RELEVANCE FOR THE NUCLEAR EQUATION OF STATE

G. Colò

Dipartimento di Fisica, Università degli Studi, and INFN, Sezione di Milano, Milano, Italy

Accurate assessment of the value of the incompressibility coefficient, K_∞, of symmetric nuclear matter, which is directly related to the curvature of the equation of state (EOS), is needed to extend our knowledge of the EOS in the vicinity of the saturation point. We review the current status of K_∞, as determined from experimental data on isoscalar giant monopole and dipole resonances (compression modes) in nuclei, by employing the microscopic theory based on the Random Phase Approximation (RPA). The importance of full self-consistent calculations is emphasized. In recent years, the comparison between RPA calculations based on either nonrelativistic effective interactions, or relativistic Lagrangians, has been pursued in great detail. It has been pointed out that these two types of models embed different ansatz for the density dependence of the symmetry energy. This fact has consequences on the extraction of the nuclear incompressibility, as it is discussed. The comparison with other ways of extracting K_∞ from experimental data is highlighted.

Точная оценка величины коэффициента несжимаемости K_∞ симметричной ядерной материи, который непосредственно связан с кривизной уравнения состояния (УС), необходима для исследования свойств УС в окрестности точки насыщения. Приводится обзор текущего представления о K_∞, который определяется из экспериментальных данных по изоскалярному гигантскому монопольному и дипольному резонансам (моды сжатия) в ядрах, при использовании микроскопической теории, основывающейся на приближении случайных фаз (ПСФ). Подчеркивается важность проведения полностью самосогласованных вычислений. За последнее время было проведено детальное сравнение ПСФ-вычислений как в модели нерелятивистских эффективных взаимодействий, так и с использованием релятивистских лагранжианов. Было установлено, что эти два типа моделей подразумевают различный анзац для зависимости энергии симметрии от плотности, что, в свою очередь, влияет на механизм извлечения величины ядерной несжимаемости. Проводится также сравнение с другими способами извлечения K_∞ из экспериментальных данных.

PACS: 21.65.+f, 24.30.Cz, 64.30.+t

INTRODUCTION

Our understanding of the structure of the ground state and the excited states of atomic nuclei, is still not fully satisfactory. At the same time, there is need of theoretical progress along this line if the existing or planned radioactive beam facilities will provide us with new experimental data. These data will concern nuclei far from the stability valley; consequently, a unified description of usual

nuclear matter as well as of neutron-rich (or proton-rich) matter will be called for.

For light systems, the so-called *ab-initio* methods, which start from the bare nucleon–nucleon (NN) interaction, can be applied. Highly sophisticated trial wave functions allow using the variational method and extracting a fairly good description of these systems. Alternatively, the so-called Green's Function Monte Carlo (GFMC) approach can be used. But all these methods cannot be applied to finite nuclei having mass number A greater than ≈ 10–15. Unfortunately, only this kind of nuclei allows determining (yet with many warnings) the basic features of the equation of state (EOS) of nuclear matter, as we discuss below.

The present review is devoted to the extraction of the nuclear incompressibility coefficient from the measurement of the compressional modes in finite nuclei. Compressional modes include the Isoscalar Giant Monopole Resonance (ISGMR) and Isoscalar Giant Dipole Resonance (ISGDR), which lie between 10 and 30 MeV in nuclei ranging from ^{90}Zr to ^{208}Pb. In these nuclei, the ISGMR corresponds really to a well-defined single peak. The ISGDR is associated with several structures, and the ambiguities which derive from this will be discussed in the following. In lighter nuclei, even the ISGMR is too much fragmented to allow discussing about a single compressional mode.

If we are, accordingly, bound to discuss relatively high-energy excitations of heavy systems, then not only the fully *ab-initio* methods that we have mentioned, but also other microscopic models like the shell model are completely ruled out. The most microscopic models that we can use are the mean field models based on effective interactions, either in the nonrelativistic or relativistic framework. These models are the theoretical basis for the analysis done in the following Sections. They can be viewed as approximate realizations of a Density Functional Theory (DFT) for atomic nuclei.

In the past, previous authors have attempted either a direct extraction of the nuclear incompressibility from experimental data (without resorting to theory), or an extraction based on other observables than the compressional modes. The limitations of these approaches are discussed below. In fact, these issues have been already discussed since ten years or more. Already in the celebrated review paper by J. P. Blaizot [1] these points have been dealt with. Further developments will be mentioned here, when discussing the relevant bibliographic references. What does it make a new review on the subject quite timely? We answer this question in this Introduction, before giving a brief outline of the following of the present paper.

Only since few years, the relativistic mean field (RMF) calculations have reached a reliability or accuracy that is comparable to that of the nonrelativistic models. During the eighties, no relativistic model could describe satisfactorily the compressional modes and the nuclear incompressibility. Later, significant

progress has been made. It has been understood that only by adding nonlinear meson self-interaction terms to the effective Lagrangian of the original Walecka model (cf. Subsec. 2.2) the incompressibility can assume reasonable values. For some time, there has been discussion about the proper way to perform relativistic Random Phase Approximation (RPA) and/or Time-Dependent Relativistic Mean Field (TDRMF) calculations, and afterwards it has been concluded that the inclusion of the negative-energy Dirac sea states is necessary. During the last years, it has been pointed out that from the relativistic mean field calculations a significantly larger value of nuclear incompressibility emerges than in the nonrelativistic framework.

This has motivated several debates. It would be not physically sound to admit that some specific effect related to special relativity comes in, since one is concerned to rather low energies (or momenta) and low densities (very close to the saturation density). In fact, for many observables ranging from nuclear masses to other types of giant resonances, and to rotational bands up to their endpoint, the nonrelativistic and relativistic pictures look very consistent with each other.

Recently, the following conclusions have been reached: (i) some previous nonrelativistic RPA calculations were not accurate enough to allow a precise determination of the nuclear incompressibility; (ii) the discrepancy between nonrelativistic and relativistic determinations of the nuclear incompressibility is associated with the detailed structure of the two classes of nuclear energy functionals. This amounts to say that there is much richer physics than it has been discussed in earlier papers on the subject, and these new aspects have emerged in recent years. This is the main motivation for the present review.

At the same time, the experimental measurements have also undergone significant progresses. The determination of the main features of the ISGMR has become much more accurate than in the past. The uncertainties about the energy location of the ISGDR have been attacked. New chains of isotopes have been measured, and some others have been measured with improved accuracy. This is an important part of the new impetus which characterizes the field. Although this is a theoretical review, we shall mention the relevant experimental papers and discuss their impact as much as possible.

In summary, the aim of this review is to assess what conclusions about the nuclear incompressibility can be reached by confronting the most recent mean field calculations — both in the nonrelativistic and relativistic versions. It will be concluded that the extraction of the incompressibility brings in other physics parameters embedded in the energy functionals, like, for instance, the associated values of the symmetry energy. Part of the results reviewed here have been already summarized in [2–4]. The present topic has been also touched upon (briefly) in [5].

The outline of the following Sections is as follows. First, we define briefly in Sec. 1 the object of our study, namely, the nuclear incompressibility K_∞ and its basic relation with the energy of symmetric nuclear matter. Then, we describe the models which give a physically sound representation of the total energy either in symmetric nuclear matter (which cannot be measured) or in finite nuclei (whose properties can be measured). These are the self-consistent mean field models: we remind their basic features in Sec. 2 and we touch briefly upon how they are used in actual calculations in Sec. 3. Having defined our tools, we turn to the main issue, namely how to relate K_∞ with some sensitive measurable quantity, in Sec. 4. We will conclude that, although other lines of research can be extremely useful, the connection of K_∞ with the ISGMR and, to some extent, the ISGDR, is by far the best case. Then, we will review the experimental situation concerning these modes in Sec. 5. The extraction of K_∞ from experiment, based on the ISGMR data in ^{208}Pb and on different RPA calculations, is analyzed in Sec. 6; and the case of other nuclei, in Sec. 7. The complementary case of the ISGDR data is then discussed in Sec. 8. Finally, we draw conclusions and propose some outlook in the last section.

1. DEFINITION OF THE NUCLEAR INCOMPRESSIBILITY

We usually define the compressibility as

$$\chi = -\frac{1}{V}\left(\frac{\partial P}{\partial V}\right)^{-1}, \tag{1}$$

and this quantity has the dimension of 1/pressure. Often, the inverse quantity χ^{-1} is considered. Values of χ^{-1} are $2.2 \cdot 10^9$ for water and $1.6 \cdot 10^{11}$ for steel if expressed by using Pascal, that is, N/m^2 (the standard international units).

We consider a system at zero temperature in which the pressure is related to the total energy E by

$$P = -\frac{\partial E}{\partial V}, \tag{2}$$

so that

$$\chi^{-1} = V\frac{\partial^2 E}{\partial V^2}. \tag{3}$$

If we introduce the density ρ as single variable and we consider the number of particles A as fixed ($\rho = A/V$), since

$$\frac{\partial}{\partial V} = -\frac{A}{V^2}\frac{d}{d\rho},$$

we obtain

$$P = \rho^2 \frac{d(E/A)}{d\rho}, \tag{4}$$

$$\chi^{-1} = \rho^3 \frac{d^2(E/A)}{d\rho^2}. \tag{5}$$

In the case of nuclear matter at zero temperature, it is preferred to introduce a quantity displaying a more direct relationship with the behavior of E/A around the saturation point. This latter is known empirically to be $\rho_0 = 0.166$ fm^{-3} and it corresponds to the minimum point of E/A. Around this minimum,

$$\frac{E}{A}(\rho) = \frac{E}{A}(\rho_0) + \frac{1}{18} K_\infty \left(\frac{\rho - \rho_0}{\rho_0} \right)^2 + \ldots, \tag{6}$$

where

$$K_\infty = 9\rho_0^2 \frac{d^2(E/A)}{d\rho^2}\bigg|_{\rho_0} \tag{7}$$

is the so-called compression modulus of nuclear matter. Sometimes it is also called nuclear incompressibility coefficient, or, briefly, nuclear incompressibility. It can be simply related to χ^{-1} by

$$K_\infty = \frac{9}{\rho_0} \chi^{-1}. \tag{8}$$

K_∞ has been defined so to have dimension of energy. Since, as we discuss in the following of this review, we accept nowadays values of K_∞ which are around 250 MeV, one can deduce that nuclear matter is 22 orders of magnitude more incompressible than steel.

Instead of the density, the Fermi momentum k_F is often used as independent variable. Since an elementary calculation shows that

$$\rho = \frac{2}{3\pi^2} k_F^3, \tag{9}$$

then Eq. (7) is equivalent to

$$K_\infty = k_F^2 \frac{d^2(E/A)}{dk_F^2}\bigg|_{k_{F\,0}}. \tag{10}$$

In fact, K_∞ has been directly associated with the curvature of E/A as a function of the Fermi momentum, and this explains the origin of the factor 9 in Eq. (7). We remind here that the empirical value of k_{F0} is 1.35 fm^{-1}.

Nuclear matter is a uniform system in which the energy per particle can be simply related to the energy density $\mathcal{E}$ by E/A=$\mathcal{E}/\rho$. Every nuclear model which provides an energy density for infinite matter, provides as well a value for the nuclear incompressibility.

2. MEAN FIELD MODELS

2.1. Nonrelativistic Effective Interactions. It appears evident from the discussion in Introduction that only models which describe at the same time finite nuclei and infinite matter, by using the density as a basic variable, can be used to attack the problem of the determination of K_∞. At present, only the mean field models are available for this aim. Nonrelativistic mean field models start from an effective interaction $V_{\rm eff}$. The expectation value of $H_{\rm eff} = T + V_{\rm eff}$ (where T is the kinetic energy) on an independent-particle type wave function (i.e., a Slater determinant) provides the energy functional $E[\rho]$.

Among the most widely used effective interactions, there are those introduced by T. H. R. Skyrme [6]. They have the form

$$\begin{aligned} V_{\rm Skyrme} = {} & t_0\,(1 + x_0 P_\sigma)\,\delta(\mathbf{r}_1 - \mathbf{r}_2) + \\ & + \frac{1}{2}\,t_1\,(1 + x_1 P_\sigma)\Big(\mathbf{k}^{\dagger 2}\,\delta(\mathbf{r}_1 - \mathbf{r}_2) + \delta(\mathbf{r}_1 - \mathbf{r}_2)\,\mathbf{k}^2\Big) + \\ & + t_2\,(1 + x_2 P_\sigma)\,\mathbf{k}^\dagger \cdot \delta(\mathbf{r}_1 - \mathbf{r}_2)\,\mathbf{k} + \\ & + \frac{1}{6}\,t_3\,(1 + x_3 P_\sigma)\,\delta(\mathbf{r}_1 - \mathbf{r}_2)\,\rho^\alpha\left(\frac{\mathbf{r}_1 + \mathbf{r}_2}{2}\right) + \\ & + iW_0\,(\sigma_1 + \sigma_2) \cdot \mathbf{k}^\dagger \times \delta(\mathbf{r}_1 - \mathbf{r}_2)\mathbf{k}, \quad (11) \end{aligned}$$

where $\mathbf{k}$ is the relative momentum operator, $\mathbf{k} = \dfrac{i}{2}\,(\nabla_1 - \nabla_2)$, and $\mathbf{k}^\dagger$ is its adjoint; P_σ is the spin-exchange operator $\left(1 + \dfrac{\sigma_1 \cdot \sigma_2}{2}\right)$. The Skyrme interaction is characterized, in its standard form, by ten adjustable parameters (t_i, x_i, α and W_0). Many parameter sets have been fitted since the pioneering works [7, 8]. Although, as it is repeated by many authors, there exist a huge number of Skyrme parameter sets available on the market, a limited number of them can perform reasonably well if they are tested against many different observables. The big advantage of a zero range force lies in the fact that it produces a local energy functional. Of course, in systems which are not spin (or isospin) saturated, spin (or isospin) densities enter the energy functional. Because of the velocity dependence other kinds of local functions (like the kinetic energy density τ, the gradient of the density $\boldsymbol{\nabla}\rho$, and the spin-orbit density $\mathbf{J}$) are involved. Therefore, although we often denote the energy functional simply as $E[\rho]$, we mean nonetheless that there is dependence on other kinds of local densities. For details, one can consult the review paper [9], where the fact that the dependence on different local densities can simulate the finite-range effects is also discussed (cf. Sec. I.D). Within the Skyrme framework, to not spoil the locality of the resulting Hartree–Fock equations, the exchange Coulomb term is often treated by using the Slater approximation.

Another kind of effective interaction is the finite-range Gogny force [10, 11], which reads

$$V_{\text{Gogny}} = \sum_{j=1}^{2} \exp\left(\frac{|\mathbf{r}_1 - \mathbf{r}_2|}{\mu_j}\right)^2 \big(W_j + B_j P_\sigma - H_j P_\tau - M_j P_\sigma P_\tau\big) + \\ + t_3\big(1 + x_0 P_\sigma\big)\delta(\mathbf{r}_1 - \mathbf{r}_2)\, \rho^\alpha\left(\frac{\mathbf{r}_1 + \mathbf{r}_2}{2}\right) + \\ + iW_0(\sigma_1 + \sigma_2) \cdot \mathbf{k}^\dagger \times \delta(\mathbf{r}_1 - \mathbf{r}_2)\, \mathbf{k}, \quad (12)$$

where P_σ has been defined above and P_τ is the analogous isospin-exchange operator. The interaction includes the sum of two Gaussians with space, spin and isospin exchange mixtures, a term with explicit density dependence, and a spin-orbit term. W_j, B_j, H_j, M_j, μ_j, t_3, x_0, α, and W_0 are the adjustable parameters of the interaction.

The Gogny interaction is meant to be used within the framework of Hartree–Fock–Bogoliubov (HFB) theory [12]. The Skyrme force is used in Hartree–Fock (HF) calculations, and extensions to the open-shell isotopes are made by supplementing it with an independent pairing force. Often a zero-range, density-dependent pairing force is introduced, whose parameters are fitted by requiring that the empirical values of the pairing gaps Δ are reproduced (along a given isotope chain). In the following of this review paper we will mainly be concerned with calculations which do not include pairing: even in the case of the Gogny force, we will mainly refer to simple HF calculations.

The parameters of the effective interactions are fitted by using as benchmark a limited number of properties of infinite matter (like the saturation point) and of finite nuclei (total energies and charge radii of few selected isotopes).

The total energy is calculated by taking the expectation value of the effective Hamiltonian

$$H = T + V_{\text{eff}} \quad (13)$$

over an independent-particle state $|\Phi\rangle$, that is, a Slater determinant,

$$E = \langle\Phi|H|\Phi\rangle. \quad (14)$$

$|\Phi\rangle$ is associated with a given one-body set of densities ρ, τ, $\mathbf{J}$ as well as their spin and isospin generalizations (in fact, if the system is described within the independent-particle approximation, the two-body density is simply factorized in terms of one-body densities).

In finite nuclei, the optimal Slater determinant emerges from the numerical solution of the HF equations. Total energies, as well as radii and expectation values of other observables, can be extracted from this solution.

The calculation of infinite matter is simpler: namely, it is analytic since the total density is simply a number and the functional is a simple function. The nuclear incompressibility (7) is straightforward to calculate and sometimes it is used as an additional constraint when fitting the force parameters. Asymmetric nuclear matter can also be calculated. When dealing with it, the energy per particle is split in a part which corresponds to symmetric matter and an asymmetry term which is taken to be quadratic in the asymmetry parameter

$$\frac{\rho_-}{\rho} \equiv \frac{\rho_n - \rho_p}{\rho},$$

where ρ_n (ρ_p) is the neutron (proton) density. The energy per particle is in fact written as

$$\frac{E}{A} = \frac{E}{A}(\rho) + S(\rho)\left(\frac{\rho_-}{\rho}\right)^2, \tag{15}$$

where the first term in the r.h.s. is the energy in symmetric matter and the second term defines the so-called symmetry energy S. The behavior of S is very much under debate, especially in connection with the study of nuclei far from stability and neutron stars (cf., e.g., [13]). Already at saturation density ρ_0, its value and its derivatives are quite uncertain; extrapolations at higher (or lower) densities are even more critical. The value of S at saturation density, $S(\rho_0)$, will be denoted by J — but other authors use the notations a_τ or a_4.

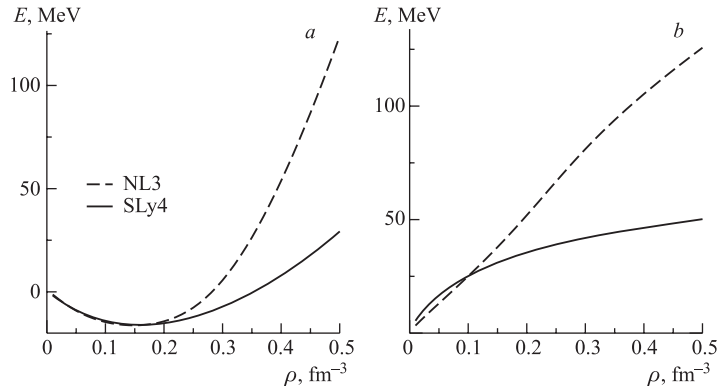

Fig. 1. Energy per particle in symmetric nuclear matter (*a*) and symmetry energy (*b*) calculated as a function of the density ρ. The results corresponding to two of the most widely used functionals, namely the Skyrme SLy4 parametrization [14] and the relativistic mean field set NL3 [15], are displayed

In Fig. 1 we compare the behavior of the total energy in symmetric matter $\frac{E}{A}(\rho)$ (Fig. 1, *a*), and of the symmetry energy $S(\rho)$ (Fig. 1, *b*), obtained by using

two different models. One is the Skyrme parameter set SLy4 introduced in [14]: it is one of the most recent sets, and it has been fitted by including the constraints which had been already taken into account for previous sets, as well as by trying to reproduce *ab-initio* calculations of pure neutron matter performed with bare forces. The other functional whose results are shown is the relativistic mean field parametrization [15], that is, the parameter set NL3. Relativistic functionals are discussed in the next subsection.

It is clear from the figure that the behavior of effective functionals well above the saturation density is far from being under control. As it can be expected, fitting the saturation properties of symmetric matter, as well as few nuclei in their ground state, cannot constrain the overall properties of the effective functionals.

2.2. The Relativistic Mean Field. In the relativistic framework, the nucleus is described in terms of Dirac particles which mutually exchange effective mesons. The simplest model of this kind, is the one introduced by B. D. Serot and J. D. Walecka twenty years ago [16]. In it, only a scalar meson σ and a vector meson ω (both isoscalar) are introduced: the first simulates the short-range attraction which in reality is made up with correlated two-pion (or more pion) exchange, while the second meson produces a repulsive effect. Saturation in nuclear matter is obtained through the balance of these very strong attractive and repulsive terms. In symmetric infinite nuclear matter, the spin and isospin terms are assumed to average out. There is no attempt to relate the masses and coupling constants of the effective mesons with more fundamental theories.

The original Walecka model is very important since it opened up the way to more systematic investigations of nuclear matter and finite nuclei. In order to describe the asymmetry degree of freedom, the isovector vector ρ meson is introduced. Besides the lack of the isovector degree of freedom, the original Walecka model suffers from other drawbacks: we mention of course, in the spirit of the present paper, the unrealistically large value of K_∞.

Nowadays, the standard finite-range meson RMF model is defined by the Lagrangian density

$$\mathcal{L} = \mathcal{L}_{\text{free nucl}} + \mathcal{L}_{\text{free meson}} + \mathcal{L}_{\text{int}}. \tag{16}$$

The first term is the Lagrangian density of the free nucleons

$$\mathcal{L}_{\text{free nucl}} = \bar{\psi}\left(i\gamma^\mu \partial_\mu - m\right)\psi, \tag{17}$$

where ψ is a Dirac spinor and m is the nucleon mass. $\mathcal{L}_{\text{free meson}}$ is the Lagrangian density of the free meson fields (and the electromagnetic field) which

reads

$$\mathcal{L}_{\text{free meson}} = \frac{1}{2}\partial_\mu\sigma\partial^\mu\sigma - \frac{1}{2}m_\sigma^2\sigma^2 - \frac{1}{4}\Omega_{\mu\nu}\Omega^{\mu\nu} + \frac{1}{2}m_\omega^2\omega_\mu\omega^\mu - \\ - \frac{1}{4}\mathbf{R}_{\mu\nu}\mathbf{R}^{\mu\nu} + \frac{1}{2}m_\rho^2\boldsymbol{\rho}_\mu\boldsymbol{\rho}^\mu - \frac{1}{4}F_{\mu\nu}F^{\mu\nu}. \quad (18)$$

In this equation, the meson masses appear with obvious notation, while $\Omega_{\mu\nu}$, $\mathbf{R}_{\mu\nu}$, and $F_{\mu\nu}$ are field tensors, i.e.,

$$\begin{aligned} \Omega_{\mu\nu} &= \partial_\mu\omega_\nu - \partial_\nu\omega_\mu, \\ \mathbf{R}_{\mu\nu} &= \partial_\mu\boldsymbol{\rho}_\nu - \partial_\nu\boldsymbol{\rho}_\mu, \\ F_{\mu\nu} &= \partial_\mu A_\nu - \partial_\nu A_\mu, \end{aligned} \quad (19)$$

where $\mathbf{R}$ and $\boldsymbol{\rho}$ are isovector quantities. The meson–nucleon interactions are included in

$$\mathcal{L}_{\text{int}} = -\bar\psi\Gamma_\sigma\sigma\psi - \bar\psi\Gamma_\omega^\mu\omega_\mu\psi - \bar\psi\boldsymbol{\Gamma}_\rho^\mu\boldsymbol{\rho}_\mu\psi - \bar\psi\Gamma_e^\mu A_\mu\psi. \quad (20)$$

The vertices read

$$\Gamma_\sigma = g_\sigma, \quad \Gamma_\omega^\mu = g_\omega\gamma^\mu, \quad \boldsymbol{\Gamma}_\rho^\mu = g_\rho\boldsymbol{\tau}\gamma^\mu, \quad \Gamma_e^\mu = e\frac{1-\tau_z}{2}\gamma^\mu, \quad (21)$$

with the coupling parameters g_σ, g_ω, g_ρ, and e.

In order to describe correctly the interactions in the nuclear medium, this model should be further improved. One way is to add nonlinear meson self-interaction terms. We can write them for the σ meson, namely

$$U(\sigma) = \frac{1}{3}g_2\sigma^3 + \frac{1}{4}g_3\sigma^4. \quad (22)$$

In this way, the free parameters are eight. An example of parameter set is the one already quoted, namely NL3.

An alternative way to take into account the medium dependence of the effective Lagrangian, is to use density-dependent coupling constants. In principle, this may allow connecting the effective Lagrangian with more basic calculations like, e.g., the Dirac–Brückner approach. In practice, however, the density dependence of the coupling constants is assumed to have a given functional form with free parameters which must be fixed. For details, the reader can consult the references quoted in [17]. One more class of models are the so-called point-coupling (PC) models, in which the mesonic degrees of freedom are integrated out and nucleon–nucleon couplings are introduced [18]. These models could be the most suitable for comparisons with the nonrelativistic Hamiltonians (in particular, with those including the Skyrme effective interaction (11)) — however, applications to the

compressional modes have been carried out by using only the finite-range meson exchange Lagrangians, or those characterized by density-dependent coupling constants. The results, to be discussed in the next sections, are in either cases of comparable quality and features.

The parameters of all models are determined in a similar way as in the nonrelativistic theories. That is, properties of nuclear matter and binding energies/charge radii of magic isotopes are used as input. The discussion carried out in the previous subsection, concerning the determination of the total energy and other properties of the ground state of finite nuclei and infinite matter, applies as well to the present case. Within the standard RMF framework, however, calculations are performed at the Hartree level.

The real advantage of the RMF models should consist in the fact that in the covariant framework, one has better hopes to get eventually contact with more fundamental theories like QCD, or one of its low-energy approximations. In fact, this has been the aim of recent works, which are anyway outside the aim of the present review. The advantage of models like Skyrme or Gogny, lies in the fact that they have been exploited for longer time and their link with the nuclear phenomenology has been more deeply established. Probably, only a severe confrontation between the two classes of approaches may shed light on basic issues of nuclear science, like the determination of the parameters of the EOS.

We conclude this subsection by reminding that, because of parity conservation, in the RMF models there is no direct contribution from the pion field at the Hartree level. Recently, there have been new attempts to implement a relativistic Hartree–Fock (RHF) scheme [19] in which the role of the pion field can be discussed. Applications to the compressional modes through relativistic RPA based on RHF have still to be performed.

3. EXCITED STATES FROM THE MEAN FIELD MODELS

HF and RPA calculations, respectively for the ground state and the vibrational excitations of nuclei, are described in textbooks [12, 20]. We already touched upon the HF formalism in the previous section. In the present section we will add some key features of the RPA calculations (those which are more relevant for the following discussion).

3.1. The Random Phase Approximation. The Random Phase Approximation (RPA) — as well as its extension to the case of open-shell nuclei, the Quasiparticle Random Phase Approximation (QRPA) — is aimed at the description of small amplitude, collective nuclear excitations. The RPA (QRPA) represents the small amplitude limit of the time-dependent HF (HFB) theory. One can start from

the time-dependent HF equations as in [12]:

$$i\hbar\frac{\partial\rho}{\partial t} = [h(t) + f(t), \rho(t)]. \tag{23}$$

In this equation an external perturbing field f is supposed to act on the nucleus. The induced density variation (which, in turn, produces a variation of the HF Hamiltonian h, since this depends on the density) is assumed to be small enough so that linear response theory can be applied. External field $f(t)$ is harmonic, that is,

$$f(t) = f\mathrm{e}^{-i\omega t} + \mathrm{h.c.}; \tag{24}$$

accordingly, the variations of the density $\delta\rho$ and of the Hamiltonian δh,

$$\delta h = \frac{\partial h}{\partial \rho}\ \delta\rho, \tag{25}$$

will carry the same frequency. The linearization of Eq. (23) leads to

$$\hbar\omega\ \delta\rho = [\delta h, \rho_0] + [h_0, \delta\rho] + [f, \rho_0], \tag{26}$$

where the subscript 0 denotes unperturbed (i.e., ground-state) quantities.

We can obtain the RPA equations in configuration space, in which the limit of zero external field is assumed (the nuclear vibrations must sustain themselves) so that the last term in the r.h.s. of Eq. (26) does not contribute. We accomplish this by taking the matrix elements of the other terms in Eq. (26) between $\langle ph|$ and $|0\rangle$, and then also between $\langle 0|$ and $|ph\rangle$, where p and h label particle and hole states, respectively. Inserting a completeness relation in terms of a sum over all configurations labeled by $p'h'$, the RPA matrix equations finally read

$$\begin{pmatrix} A_{ph,p'h'} & B_{ph,p'h'} \\ -B_{ph,p'h'} & -A_{ph,p'h'} \end{pmatrix} \begin{pmatrix} X_{p'h'} \\ Y_{p'h'} \end{pmatrix} = E \begin{pmatrix} X_{ph} \\ Y_{ph} \end{pmatrix}. \tag{27}$$

A and B are defined as

$$\begin{aligned} A_{ph,p'h'} &= (\varepsilon_p - \varepsilon_h)\,\delta(pp')\delta(hh') + \frac{\partial h_{ph}}{\partial \rho_{ph}}, \\ B_{ph,p'h'} &= \frac{\partial h_{ph}}{\partial \rho_{hp}}, \end{aligned} \tag{28}$$

where ε are HF energies. Here and in the following of this review, we refer to self-consistent calculations as those in which the residual interaction is derived from the mean field Hamiltonian h according to the above formulas, without approximations.

The solution of the eigenvalue problem (27) determines the energies E_n of the excited vibrational states $|n\rangle$ and the corresponding wave functions expressed in terms of the so-called forward and backward amplitudes $X_{ph}^{(n)}$ and $Y_{ph}^{(n)}$,

$$|n\rangle = \sum_{ph} \left(X_{ph}^{(n)} a_p^\dagger a_h + Y_{ph}^{(n)} a_h^\dagger a_p \right) |0\rangle, \tag{29}$$

where $a^\dagger$ (a) is a creation (annihliation) operator. In spherical nuclei (we do not discuss deformed systems in the present review), the RPA equations are expressed in the angular momentum coupled representation: that is, they are written in a subspace with given angular momentum and parity, J^π. The principal source of arbitrariness in the matrix representation of RPA is the truncation of the basis. In realistic applications it is, therefore, necessary to verify the stability of the results with respect to variations of parameters that determine the discretization and truncation of the basis. The discretization can be realized by using a harmonic oscillator expansion or by setting the nucleus inside a box; the harmonic oscillator parameter or the box size are numerical parameters, as well as the upper energy limit for unperturbed energies of the ph configurations (often referred to as «energy cutoff»).

The strength function associated with the excitation operator F is defined as

$$S(E) = \sum_n |\langle n|F|0\rangle|^2 \delta(E - E_n). \tag{30}$$

The value of the transition amplitude $\langle n|F|0\rangle$ depends on the collectivity of the state $|n\rangle$ which is expressed by the X and Y amplitudes. Somewhat equivalent information is provided, in the coordinate space, by the so-called transition density of the state $|n\rangle$, which is defined as the off-diagonal matrix element of the density operator,

$$\delta\rho^{(n)}(\mathbf{r}) = \langle n| \sum_i \delta(\mathbf{r} - \mathbf{r}_i)|0\rangle. \tag{31}$$

Assuming spherical symmetry, the transition density reads

$$\delta\rho_{JM}^{(n)}(\mathbf{r}) = \delta\rho_J^{(n)}(r) Y_{JM}^*(\hat{r}). \tag{32}$$

There exists alternative formulations of RPA. In the Green-function approach [21], one evaluates the RPA Green function G, given by

$$G = G_0(1 + VG_0)^{-1}, \tag{33}$$

where G_0 is the free ph Green function and V is the residual interaction defined, as above, by

$$V(\mathbf{r}_1, \mathbf{r}_2) = \frac{\delta h(\mathbf{r}_1)}{\delta\rho(\mathbf{r}_2)}. \tag{34}$$

The Green function approach allows treating the continuum in a proper way. Although the exact solution of RPA in the continuum may be crucial if one treats weakly bound nuclei or if one is interested in the particle decay of states which lie above the threshold, discrete RPA can nonetheless reproduce the main integral properties of giant resonances in stable nuclei.

3.2. Operators and Sum Rules. In the case of the isoscalar monopole excitation, we deal with the operator

$$F_{\text{monopole}} = \sum_{i=1}^{A} r_i^2. \tag{35}$$

This operator does not carry any angular momentum, that is, it corresponds to $J^\pi = 0^+$. The macroscopic picture for a state excited by this operator, is that of an overall compression of the whole nucleus (the so-called «breathing mode»). As we will see, this macroscopic picture is, to some extent, reasonable in nuclei like ^{208}Pb where the monopole strength function is associated with a single peak (whereas it breaks in lighter nuclei).

In the case of the $J^\pi = 1^+$ isoscalar dipole, the operator is

$$F_{\text{dipole}} = \sum_{i=1}^{A} r_i^3 Y_{1m}(\hat{r}_i). \tag{36}$$

This is the so-called «overtone» with respect to

$$F_{\text{transl}} = \sum_{i=1}^{A} r_i Y_{1m}(\hat{r}_i) \tag{37}$$

which corresponds to a translation of the whole system and, consequently, is not associated with any internal excitation. The spurious translational state, which should collect all the strength of the operator (37) and should lie at zero energy, is discussed in the next Subsec. 3.3. The macroscopic picture associated with the isoscalar dipole excitation operator (36) corresponds to a nonisotropic compression mode. It is hard to take this picture literally, in view of the large degree of fragmentation displayed by the spectrum of all nuclei which have been studied.

In both cases (monopole and dipole), our discussion below will rely heavily on considerations concerning moments of the strength function (30), or sum rules. These moments are defined as

$$m_k = \int dE\ E^k S(E). \tag{38}$$

The nonenergy-weighted sum rule m_0 and energy-weighted sum rule m_1 define the centroid energy

$$E_0 = \frac{m_1}{m_0}. \tag{39}$$

The energy-weighted sum rule (EWSR) is very important because it can be shown (at least in the case of nonrelativistic RPA or QRPA) that its value equals one half of the ground-state expectation value of the double commutator

$$m_1 = \frac{1}{2}[F,[H,F]]. \tag{40}$$

This is the well-known Thouless theorem, which has been shown to hold in the case of self-consistent HF plus RPA calculations (and also HFB plus QRPA).

In addition to E_0, another quantity which can be defined is what is called often constrained energy, namely

$$E_{-1} = \sqrt{\frac{m_1}{m_{-1}}}. \tag{41}$$

Its interest derives from the fact that it can be derived without resorting to a full RPA calculation: m_1 can be taken from the double commutator (40), and m_{-1}, from the so-called dielectric theorem [22]. If one performs a constrained Hartree–Fock (CHF) calculation, that is, if one minimizes the expectation value of

$$H + \lambda F, \tag{42}$$

where λ is a Lagrange multiplier, then it can be shown that

$$m_{-1} = -\frac{1}{2}\frac{\partial\langle F\rangle}{\partial\lambda} = \frac{1}{2}\frac{\partial^2\langle H\rangle}{\partial\lambda^2}. \tag{43}$$

In order to obtain accurate values of the above-mentioned sum rules and, in particular, to respect the Thouless theorem and the dielectric theorem, full self-consistency is quite important. We repeat here that self-consistency means, in the present context, that the ph interaction to be used in RPA is derived from the mean field without any approximation. Only recently, full self-consistent calculations using the Skyrme interaction have become available [23–28]. Previously, some terms of the residual ph interaction were usually neglected: in most cases, the two-body Coulomb and two-body spin-orbit terms. As we discuss in Sec. 6, this approximation affects the ISGMR centroid energies by few hundreds of keV and this has consequences on the determination of K_∞.

Of course, other kind of approximations are involved in the actual implementation of RPA. So, one may wonder if these approximations (like the continuum discretization, the model space truncation and the numerical uncertainties) affect as well the values of the RPA sum rules. In [2], it has been already mentioned (cf. Table 1) that those approximations do not affect the accuracy with which the dielectric theorem is satisfied by more than about 1%.

In Fig. 2, we show our results for the monopole centroid energies in the case of ^{40}Ca (obtained by employing the force SLy4 [14]). The results are

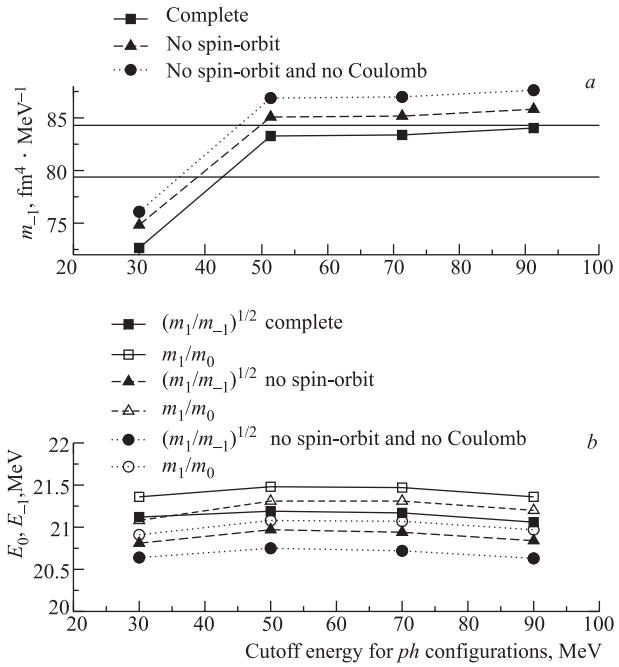

Fig. 2. *a*) Values of m_{-1} from RPA calculations, within different approximations, compared with the «exact» value from the dielectric theorem (43) which corresponds to the area between the horizontal lines. *b*) Values of the energies E_0 and E_{-1}. All values refer to ^{40}Ca calculated with the Skyrme force SLy4, and are functions of the cutoff energy set in the RPA calculation

shown as a function of the energy cutoff for the particle-hole configurations. In Fig. 2, *a* the CHF value for m_{-1}, with a numerical error bar*, is marked by the two horizontal lines. Only the calculation with the full residual interaction (labelled by «Complete») lies within this range. When the two-body Coulomb and spin-orbit terms in the residual ph force are omitted, the m_{-1} sum rule is overestimated. To provide another example, in the case of ^{208}Pb with the interaction SGII [29], and employing a box of 20 fm, the value of m_{-1} from RPA is 226.32 fm^4/MeV, in excellent agreement with the result from CHF which is 225.92 fm^4/MeV.

*If m_{-1} has to be extracted from Eq. (43), an extremely small value of λ has to be employed, so that the variations involved are subject to percentual errors of a few %.

We end this subsection by mentioning another quantity that is sometimes used, namely the so-called scaled energy,

$$E_3 = \sqrt{\frac{m_3}{m_1}}. \tag{44}$$

Also in this case, we refer the reader to [22] for details. The cubic energy-weighted sum rule m_3 can be calculated by making the following transformation on the ground-state wave function,

$$|0\rangle \ \rightarrow |\lambda\rangle \equiv \mathrm{e}^{\lambda[H,F]}|0\rangle, \tag{45}$$

where λ is a real parameter. Then

$$m_3 = \frac{\partial^2}{\partial\lambda^2}\,\langle\lambda|H|\lambda\rangle|_{\lambda=0}\,. \tag{46}$$

In the case of the Skyrme Hamiltonian, when F is the monopole operator (35), one can derive the following expression:

$$m_3 = \frac{2}{m^2}\left[2T + E_\delta + 20\,(E_{\mathrm{fin}} + E_{\mathrm{s.o}}) + (3\alpha+2)\,(3\alpha+3)\,E_\rho\right], \tag{47}$$

where the quantities T, E_δ, E_{fin}, $E_{\mathrm{s.o}}$, and E_ρ are, respectively, the contributions to the ground-state HF energy arising from the kinetic part, the t_0 part of the two-body interaction, the t_1 and t_2 terms, the spin-orbit and the t_3 contributions (cf. Eq. (11)). Their expressions can be found in [22]. We do not discuss the derivation of m_3 in detail, since we will not use the scaled energy in the further discussion. The main reason is that m_3 is clearly sensitive to high-lying strength and if one wishes to compare with experiment, one needs to remember that high-lying strength lies in a region of very large background. This makes the experimental extraction of m_3 rather questionable.

We end this subsection by referring the reader also to [30] in order to find deep and complete discussions on the sum rules and their role in the analysis of collective vibrational states.

3.3. The Spurious Dipole State. It is well known that the mean field solution of the nuclear Hamiltonian, although rather successful in practice, breaks important symmetries (cf., e.g., Chapter 11 of [12]). One of these symmetries, strictly related with the discussion of the present paper, is the translational symmetry. Of course, this symmetry is inherent in the nuclear Hamiltonian; but the HF solution breaks it, in keeping with the fact that it is a localized solution. Many discussions have been devoted to this problem, and accounting for all of them is well beyond our purpose here. We merely quote that it has been demonstrated that within an ideal, fully self-consistent HF-RPA calculation, the translational symmetry must

be fully restored [31]. This means that the whole strength of the operator (37) should be concentrated in a single state lying at zero energy. This state is called spurious since it does not correspond to any excitation of the system.

This ideal symmetry restoration could be obtained if practical calculations were implemented without any approximation. This hypothetical condition is of course never met. In practice, the spurious state is found at energy different from zero, and it is not orthogonal to the other, physical states. The position in energy is not a serious problem. In fact, a small renormalization of the residual interaction (achieved by multiplying the residual ph interaction by a parameter g_{ph} which differs only by few percent from one) can set the state arbitrarily close to zero, which means few eV in actual calculations. Anyway, even if the spurious state remains at few hundreds keV, it can be easily identified if it exhausts most of the strength of the operator (37), and eliminated from the IS dipole spectrum. But the real problem comes from the fact that since the wave function of this nonideal, inaccurate spurious state does not coincide with that of the true spurious state, part of the spurious components are found in the other dipole states. Then, the whole dipole spectrum must be corrected.

One possible solution consists in projecting away explicitly the spurious components from every state, before calculating its strength. The spurious state exact wave function is known. In configuration space, its X and Y components are, respectively, the ph and hp matrix elements of the total momentum operator (cf., e.g., [32]). Its radial transition density, $\delta\rho_{1^-}^{(\mathrm{spurious})}(r)$ (cf. Eq. (32)), is proportional to the radial derivative of the ground-state density, $d\rho_0/dr$ [33]. If we call $|\mathrm{SS}\rangle$ the wave function of the (exact) spurious state, starting from the RPA eigenstates $|n\rangle$, it is possible to build a new set of states $|n'\rangle$ in which the spurious component has been removed (cf. also [34]). We write

$$|n'\rangle = \mathcal{N}\left(|n\rangle - a_n|\mathrm{SS}\rangle\right), \tag{48}$$

where $\mathcal{N}$ is a normalization constant. The unknown quantity a_n is found by imposing that the state $|n'\rangle$ carries no strength associated with the translational operator (37), that is,

$$\langle n'|F_{\mathrm{transl}}|0\rangle = 0. \tag{49}$$

An equivalent procedure [35] consists in using instead of (36) the modified operator

$$F_{\mathrm{dipole}}^{(\mathrm{eff})} = \sum_{i=1}^{A}\left(r_i^3 - \eta r_i\right) Y_{1m}(\hat{r}_i), \tag{50}$$

where $\eta = \dfrac{5}{3}\langle r^2\rangle$. Both procedures should ensure that the calculated strength function is free from spurious components (cf. also the related deep discussions in [36, 37]).

4. EXTRACTION OF THE NUCLEAR INCOMPRESSIBILITY

4.1. The General Framework. Many attempts have been done to extract the correct value of the nuclear incompressibility. This quantity cannot be determined directly by means of experiment. Theory should provide a clear correlation between the value of K_∞ and the value of some other observable which can be directly measured. We briefly review, in what follows, different approaches along these lines and underline their limits.

In [38], it was concluded that neither nuclear masses, nor nuclear radii, nor heavy-ion collisions, nor neutron stars, are able to provide error bars smaller than 50–100 MeV on K_∞: they basically leave this quantity free in the large interval $\approx$ 200–300 MeV. But, according to [38], the supernova explosion would require lower values of K_∞ (below $\approx$ 180 MeV). On the other hand, the authors of [39] claim that a quite accurate value of K_∞ can be extracted from their fit of a Thomas–Fermi model for cold nuclear matter. This value, $K_\infty = 234$ MeV, is quite similar to those deduced from the ISGMR using standard Skyrme and Gogny interactions. The liquid drop model (LDM) expansions of binding energy and incompressibility carried out in [40] lead instead to $K_\infty = (288 \pm 20)$ MeV.

While it is certainly true that one should aim at a unified understanding of the nuclear EOS, so that all physical quantities can be extracted from a unique set of parameters of this EOS, the present short discussion already highlights the fact that this global and ambitious goal has not yet been reached. In fact, in the case of many of the observables which have been mentioned, there is not a definite correlation with the value of K_∞. One might argue that the realistic values of the observables can be reproduced by changing the value of K_∞ *and, at the same time,* some other of the different parameters which enter the nuclear EOS. Before trying to state a conclusion about the proper value of K_∞, one should prove a) that there is a clear-cut correlation between a given observable and the value of K_∞, and b) what changes if other ingredients of the model are changed.

In this respect, the situation is much advanced concerning the correlation between K_∞ and the energies of the compression modes which characterize the finite nuclei, especially the ISGMR. In fact, it was first proven in [41] that, within the mean field calculations, the correlation between the ISGMR energy and K_∞ is quite clear and accurate, at least in nuclei like Sn and Pb. However, as mentioned in Introduction, when the RMF calculations have become available, it was proven that the correlation between K_∞ and the ISGMR energy is present in these models as well, but points to a different value of K_∞ as compared to the nonrelativistic case. This issue will be the focus of the discussions carried out in the next sections.

Before entering into details of the relationship between the energies of the compressional modes and K_∞, we should mention that independent attempts of finding a unique correlation between K_∞ and selected experimental data have

been done by studying in detail specific cases of nuclear reactions. The simplest case is elastic scattering. Intermediate energy proton–nucleus or nucleus–nucleus collisions (at several tenths of MeV per nucleon) can be studied microscopically by using the Distorted Wave Born Approximation (DWBA). Microscopic NN interactions can be used within the framework of the folding model. Starting from the original M3Y interaction developed by the Michigan group, interactions which do include a density dependence have been developed. These interactions are able to provide saturation of nuclear matter, and realistic values of K_∞. The authors of [42, 43] have shown that the study of α nucleus and nucleus–nucleus refractive scattering is instrumental to determine the value of K_∞. The values of K_∞ associated with the parameter sets which reproduce those experimental elastic scattering differential cross sections, namely K_∞ around 230–260 MeV, are quite similar to those extracted from the ISGMR and discussed below.

At the other extreme of the variety of nuclear reactions, compared to the «gentle» case of elastic scattering, we find high-energy heavy-ion collisions. The many observables which can be extracted from these experiments can be analyzed by means of transport models. They also include, through the NN interaction or in some equivalent way, basic parameters of the EOS like the nuclear incompressibility. Therefore, one can study what value of K_∞ can be extracted (see, e.g., [44]). In this case, the conclusions reached by different groups do not converge yet to a narrow interval of values of K_∞.

4.2. The Extraction from Compressional Modes: Macroscopic Approaches. Well before the correlation shown in [41] between the RPA monopole energies and the value of K_∞, much attention had been paid to the possibility to link this latter quantity and the breathing mode properties. The energies of the breathing mode are measured in finite nuclei. If there are not ambiguities about the value of $E_{\rm ISGMR}$, there is nonetheless a well definite problem in relating this energy and the corresponding incompressibility of the finite system with the value of K_∞.

As we discuss in the next section, the monopole strength distributions have been measured in many nuclei, ranging from the very light to the heavy ones. In fact, what is measured is the reaction cross section and we assume, for the moment, that there exists (at least approximately) a proportionality between cross sections and monopole strength (this topic is discussed in Sec. 5). Light nuclei are not at all suited for the extraction of the incompressibility, as the cross section, or strength distributions, look highly fragmented. The result of a theoretical calculation of the monopole strength function in ^{40}Ca, done within HF-RPA employing the SLy5 Skyrme force, is displayed in Fig. 3. Clearly, it is not possible to identify a single value of energy as $E_{\rm ISGMR}$. We need cases in which the monopole strength is associated with a single peak. The ^{208}Pb isotope is, in this sense, a favourable case; also the Sn isotopes display the same feature.

In finite nuclei we cannot define the incompressibility according to (7). The density is not a number but a function of $\mathbf{r}$ and the energy per particle is a

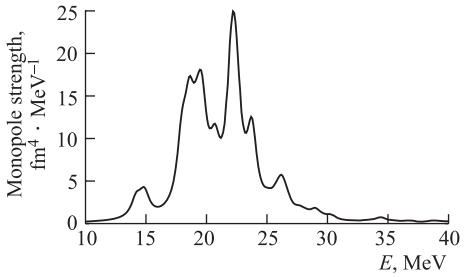

Fig. 3. Monopole strength function, calculated using RPA with the Skyrme force SLy5 [14] in the nucleus ^{40}Ca. The fragmentation of the strength is evident: it is not possible to identify a single energy value as associated to the collective ISGMR

functional. However, we can consider a simple variation of the density, that is, a variation only of its second moment $\langle r^2 \rangle$. Accordingly, we transform the derivative with respect to ρ in Eq. (7) first into a derivative with respect to the volume V, and then with respect to $\langle r^2 \rangle$. The result is

$$K_{\rm A} = 4\langle r^2 \rangle_0^2 \frac{d^2(E/A)}{d\langle r^2 \rangle^2}\bigg|_{\langle r^2 \rangle_0}. \tag{51}$$

If we write

$$H' = H + \lambda F, \tag{52}$$

where F is a generic operator, and we minimize the expectation value of H' for a fixed value of λ, then

$$\frac{d\langle H' \rangle}{d\langle F \rangle} = 0 = \frac{d\langle H \rangle}{d\langle F \rangle} + \lambda \Rightarrow \frac{d\langle H \rangle}{d\langle F \rangle} = -\lambda. \tag{53}$$

We denote $\langle H \rangle$ by E, and the above equation together with the dielectric theorem (43) implies

$$\frac{d^2E}{d\langle F \rangle^2} = -\frac{d\lambda}{d\langle F \rangle} = -\left(\frac{d\langle F \rangle}{d\lambda}\right)^{-1} = \frac{1}{2m_{-1}}. \tag{54}$$

If we specialize to $F = \sum_i r_i^2$ as in Eq. (35), and we consider that the corresponding EWSR is

$$m_1 = \frac{2\hbar^2}{m}\langle r^2 \rangle_0, \tag{55}$$

as it can be easily proven by evaluating the double commutator (40), then

$$K_A = 4\langle r^2\rangle_0^2 \left.\frac{d^2(E/A)}{d\langle r^2\rangle^2}\right|_{\langle r^2\rangle_0} = \frac{2\langle r^2\rangle_0^2}{Am_{-1}} = \frac{m\langle r^2\rangle_0}{A\hbar^2}\frac{m_1}{m_{-1}}. \tag{56}$$

If we identify the constrained energy, whose squared value m_1/m_{-1} appears in the above formula, with E_{ISGMR}, then

$$E_{\mathrm{ISGMR}} = \sqrt{\frac{\hbar^2 A K_A}{m\langle r^2\rangle_0}} \tag{57}$$

as in Eq. (3.48) of [1]. The identification of the monopole energy with the constrained energy does make sense, as it has been stressed above, if there is a single monopole peak and no fragmentation of the monopole strength.

In the macroscopic approach, K_∞ can be viewed as the leading term of an expansion of K_A as a function of A. In keeping with the associated quadratic relationship (57) between K_∞ and E_{ISGMR}, the relative error on K_∞ is twice the relative error on the monopole energy,

$$\frac{\delta K_\infty}{K_\infty} \sim 2\frac{\delta E}{E}. \tag{58}$$

There have been indeed several attempts [45] in the past to determine K_∞ simply by the following procedure. A semiempirical expansion in power of $A^{-1/3}$ of the nucleus incompressibility coefficient, K_A, has been assumed:

$$K_A = K_\infty + K_{\mathrm{surf}}A^{-1/3} + K_{\mathrm{curv}}A^{-2/3} + \\ + \left(K_\tau + K_{\tau,\mathrm{surf}}A^{-1/3}\right)\delta^2 + K_{\mathrm{Coul}}Z^2A^{-4/3} + \ldots \tag{59}$$

This expansion is analogous to the semiempirical mass formula and includes, in addition to the volume term (K_∞), surface, curvature, symmetry, and Coulomb terms (in the formula, $\delta = (N-Z)/A$). Using values of K_A associated with the experimental data of various sets of nuclei, Eq. (59) has been used for a least-square fit of the unknown coefficients of the r.h.s. All these attempts have proven to be unsatisfactory: the ISGMR data are few, and the parameters may hide correlations among themselves (cf. also [46]).

We should mention that also *theoretical approaches* along the line of Eq. (59) have been tried. In [47], Thomas–Fermi calculations have been performed for nuclei with very large A by using Skyrme forces, in an attempt to analyze both the convergence of K_∞ to its expected value, and the behavior of the other parameters included in (59). Unfortunately, it has been shown that such an analysis requires values of A which are larger than several thousands.

4.3. Microscopic Approaches. Given the difficulty mentioned in the previous subsection, namely the impossibility of getting accurate values of K_∞ from the fit of the coefficients of Eq. (59), more microscopic approaches are nowadays preferred. It is generally believed that the link between the monopole energy and K_∞ should be provided by the microscopic energy functionals. A functional (or a class of functionals) is associated with the value of K_∞, as well as with values of monopole energies in finite nuclei obtained by means of self-consistent HF plus RPA calculations (or Hartree plus RPA in the case of the RMF framework). For different nuclei, it has been shown that $E_{\rm ISGMR}$ is well correlated with the value of K_∞ associated with the effective functional (cf., e.g., [41, 48]). In connection with the experimental findings, this correlation can be used to extract an accurate value for K_∞.

In fact, this extraction proceeds as follows.

• Using a set of different parametrizations (within a given class of energy functionals) characterized by different values of K_∞, self-consistent RPA calculations of the ISGMR are performed in a given nucleus. If the monopole strength has only one peak, the quantity $E_{\rm ISGMR}$ is well defined and a relation of the type

$$E_{\rm ISGMR} = a\sqrt{K_\infty} + b \tag{60}$$

is interpolated*.

• The experimental value of $E_{\rm ISGMR}$ is then inserted in Eq. (60) and the value of K_∞ is deduced.

4.4. Is the Microscopic Approach Completely Sound? The nuclei which can be chosen in order to make the link between the monopole energy and K_∞, through the concept of an energy functional, must be not superfluid: the pairing part of the functional has not been taken into account in our previous considerations. This explains why most of the works carried out so far have been focused essentially on ^{208}Pb.

Even in this case, criticisms about the soundness of the procedure described in the previous subsection can be raised, mainly because the mean-field approximation is known to be unable to provide a complete description of the nuclear

*The interpolation should be guided by the above equation (59), so that one should better write

$$K_A = a' K_\infty + b'. \tag{61}$$

But, for instance, in [41], the explicit form of Eq. (61) in the case of ^{208}Pb is given by $K_A = 0.64K_\infty - 3.5$ (MeV). The second term of the r.h.s. is much smaller than the first term. Consequently, even if in principle the last formula together with Eq. (57) would lead to $E_{\rm ISGMR} = 1.16\sqrt{0.64K_\infty - 3.5}$, this latter equation can be approximated by $0.93\sqrt{K_\infty}$, by neglecting the second term under the square root. This explains why, in most cases, Eq. (60) is employed: in practice, Eqs. (60) and (61) are equivalent.

dynamics. The spreading width of the ISGMR can only be explained if the coupling of the RPA states with more complicated configurations of 2 particle–2 hole ($2p-2h$) type, is considered.

One reason why we believe that the discussion carried out so far is physically sound, is that it has been shown in [49] that inclusion of the mentioned coupling shifts the ISGMR in ^{208}Pb downwards in energy only by $\approx$ 500 keV (reproducing at the same time the ISGMR width), and this latter number is smaller than the uncertainties on the ISGMR energy which are discussed in the next section. This is not a numerical accident, rather a consequence of cancellations which arise when all diagrams corresponding to the coupling between $1p-h$ and $2p-2h$ states are included (cf. [50] and references therein).

There is a more fundamental point to mention here. If we wished to discuss the ISGMR in finite nuclei by using an approach similar to that of [49] (which couples the ISGMR with states including a $1p-1h$ pair plus a collective, mainly surface, vibration), we should describe the infinite matter and its compressibility at the same level. Such a scheme has not yet been developed.

5. EXPERIMENTAL EVIDENCE ON THE ISGMR AND ISGDR

In the last three decades, a significant amount of experimental work has been carried out to identify the properties of the compressional modes, the ISGMR and ISGDR. The main experimental tool is α-particle inelastic scattering. In fact, α particles are very selective in exciting states with no variation of S and T in the target nucleus ($\Delta S = \Delta T = 0$). The aim is the precise determination of the strength distribution or at least of its main moments. Since the beginning, the main obstacles to this precise determination have been the presence of other multipole excitations in the same energy region as well as of a nonnegligible background.

In the case of the ISGMR ($\Delta L = 0$), the angular distribution is strongly peaked at 0°. The recent experimental developments have made it possible to determine E_0 (cf. Eq. (39)) with an error of $\approx 0.1-0.3$ MeV [51, 52]. Using the relation (58), and the experimental energy of the ISGMR in ^{208}Pb, $E_0 = (13.96 \pm 0.20)$ MeV, one has an uncertainty of 6–9 MeV on K_∞. We point out here that the theoretical calculations have an associated error which should also be added (quadratically) to the experimental error. If we estimate this error to be also of the order of 0.2 MeV as in [2], then the total uncertainty on K_∞ is obtained by summing quadratically the two independent ones, and one gets 8–13 MeV.

The ISGMR has been identified in many nuclei, from the light to the heavy ones. In the light nuclei the strength is very fragmented and only in the medium-heavy nuclei it corresponds to a single peak of energy $\sim 80A^{-1/3}$ MeV.

The main issue here is not the experimental accuracy, rather the level of comparison between experiment and theory. Whereas, as it is discussed above (cf. Sec. 3), it is customary in the theoretical works to calculate the strength function $S(E)$, in the analysis of experimental data of the excitation cross section $\sigma(E)$ one carries out Distorted Wave Born Approximation (DWBA) calculations with a transition potential δU obtained from a collective model transition density $\delta\rho_{\rm coll}$, using the folding model (FM) approximation. This may be a source of uncertainties, especially if most of the strength is not collective. Accordingly, it is important to examine the relation between $S(E)$ and the excitation cross section $\sigma(E)$ of the ISGMR and the ISGDR, obtained by α scattering, using the folding model DWBA method with $\delta\rho$ obtained from self-consistent HF-RPA.

The DWBA has been quite instrumental in providing a theoretical description of low-energy scattering reactions and is widely used in analyzing measured cross sections of scattered probes. The folding model approach [53] to the evaluation of optical potentials appears to be quite successful and, at present, is extensively used in theoretical descriptions of α-particle scattering [54]. The main advantage of this approach is that it provides a direct link to the description of α-particle scattering reactions based on microscopic HF-RPA results.

The DWBA differential cross section for the excitation of a giant resonance by inelastic α scattering is

$$\frac{d\sigma^{\rm DWBA}}{d\Omega} = \left(\frac{\mu}{2\pi\hbar^2}\right)^2 \frac{k_f}{k_i} \left|T_{fi}\right|^2 , \tag{62}$$

where μ is the reduced mass, and k_i and k_f are the initial and final linear momenta of the α-nucleus relative motion, respectively. The transition matrix element T_{fi} is given by

$$T_{fi} = \langle \chi_f^{(-)} \Psi_f | V | \chi_i^{(+)} \Psi_i \rangle, \tag{63}$$

where V is the α-nucleon interaction; Ψ_i and Ψ_f are the initial and final states of the nucleus, and $\chi_i^{(+)}$ and $\chi_f^{(-)}$ are the corresponding distorted wave functions of the α-nucleus relative motion, respectively. To calculate T_{fi}, Eq. (63), one can adopt the following approach which is usually employed by experimentalists. First, assuming that Ψ_i and Ψ_f are known, the integrals in (63) over the coordinates of the nucleons are carried out to obtain the transition potential $\delta U \sim \int \Psi_f^* V \Psi_i$. Second, the cross section (62) is calculated using a certain DWBA code with δU and the optical potential $U(r)$ as input.

Within the FM approach, the optical potential $U(r)$ is given by

$$U(r) = \int d\mathbf{r}' V(|\ \mathbf{r} - \mathbf{r}'|, \rho_0(r'))\rho_0(r'), \tag{64}$$

where $V(|\ \mathbf{r} - \mathbf{r}'|, \rho_0(r'))$ is the α-nucleon interaction, which is generally complex and density-dependent, and $\rho_0(r')$ is the ground state HF density of a spherical

target nucleus. To obtain the results given in the following, both the real and imaginary parts of the α-nucleon interaction were chosen to have Gaussian forms with density dependence [54], and parameters determined by a fit to the elastic scattering data. The radial form $\delta U_L(r,E)$ of the transition potential, for a state with the multipolarity L and excitation energy E, is obtained from:

$$\delta U(r,E) = \int d\mathbf{r}' \delta\rho_L(\mathbf{r}',E) \Bigg[V(\mid \mathbf{r}-\mathbf{r}' \mid, \rho_0(r^{'}))+ \\ + \rho_0(r') \frac{\partial V(\mid \mathbf{r}-\mathbf{r}' \mid, \rho_0(r'))}{\partial \rho_0(r')} \Bigg], \quad (65)$$

where $\delta\rho_L(\mathbf{r}',E)$ is here the transition density for the considered state (with a slight change of notation compared to our previous discussion).

We point out that within the «microscopic» folding model approach to the α-nucleus scattering, both ρ_0 and $\delta\rho_L$, which enter Eqs. (64) and (65), are obtained from the self-consistent HF-RPA calculations. Within the «macroscopic» approach, one adopts collective transition densities, $\delta\rho_{\rm coll}$, which are assumed to have energy-independent radial shapes and are obtained using a collective model. We stress that for a proper comparison between experimental and theoretical results for $S(E)$, one should adopt the «microscopic» folding model approach in the DWBA calculations of $\sigma(E)$.

6. NUCLEAR INCOMPRESSIBILITY FROM THE ISGMR IN ^{208}Pb

The first experimental identification of the ISGMR in ^{208}Pb at excitation energy of $E_0 = 13.7$ MeV already triggered HF plus RPA calculations using existing or modified effective interactions. Those having $K_\infty = (210 \pm 30)$ MeV gave results in agreement with experiment [1]. However, in these early investigations, the experimental uncertainties for E_0 were relatively large, and especially, only a limited class of effective interactions is explored. The RMF framework was not available for confrontation with Skyrme or Gogny calculations, and many of these latter calculations were not fully self-consistent. Consequently, we accept nowadays larger values for K_∞ extracted from ^{208}Pb, as we discuss in detail in this section.

In recent years, it was clarified that relativistic RPA calculations must be performed with the inclusion of the negative-energy states of the Dirac sea. These calculations [56] yield a value of $K_\infty = 250-270$ MeV, as one can see in Fig. 4. They are performed by using Lagrangians with density-dependent meson–nucleon coupling constants. They confirm results previously obtained within the framework of the Lagrangians having density-independent coupling

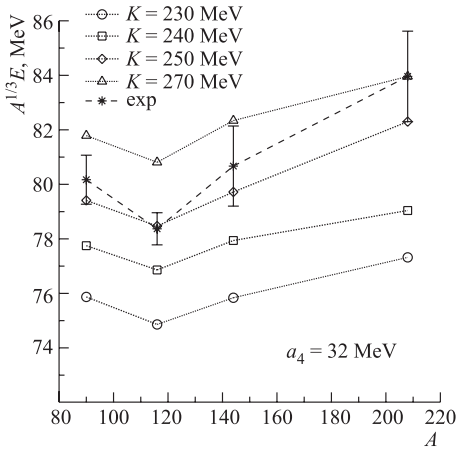

Fig. 4. Results for the ISGMR calculated within RRPA or RQRPA in different nuclei. Effective Lagrangians with density-dependent meson–nucleon vertex functions have been employed. Taken from [56]

constants and nonlinear meson self-interactions [55]. At the same time, both continuum [57] and discrete [58] HF-RPA calclations based on Skyrme still confirmed the previous result of K_∞ about 220 MeV. Note that, in keeping with an expected total uncertainty on K_∞ of about 8–13 MeV (mentioned previously in Sec. 5), a discrepancy in the predictions from relativistic and nonrelativistic models of 30–50 MeV is quite significant. This model dependence of K_∞ has been explained, to a good extent, in the most recent works of [2, 59, 60].

First, the effects of common violations of self-consistency in the HF-RPA calculations of various giant resonances were investigated in detail (cf., e.g., [23–28]). The main source of self-consistency violation is the neglect of the spin-orbit and Coulomb terms in the residual interaction. Other approximations which are usually made in the HF-RPA framework (continuum discretization, model space truncation) have been proven to be not crucial and to not produce additional inaccuracies, as discussed in Sec. 3. It is found that the effects of the violation due to the neglect of the $p-h$ spin-orbit or Coulomb interactions in the RPA calculations are most significant for the ISGMR. In ^{208}Pb the shift in the centroid energy E_0 is about 0.8 MeV, which is 3 times larger than the experimental uncertainty (cf. [2, 27]). We note that a shift of 0.8 MeV in E_0 corresponds to a shift of about 25 MeV in K_∞. In fact, this shift completely solves the issue of a previously advocated disagreement between values of K_∞ extracted from Skyrme and Gogny calculations. Fully self-consistent Skyrme calculations employing existing parameterizations do not point any more to the value of about

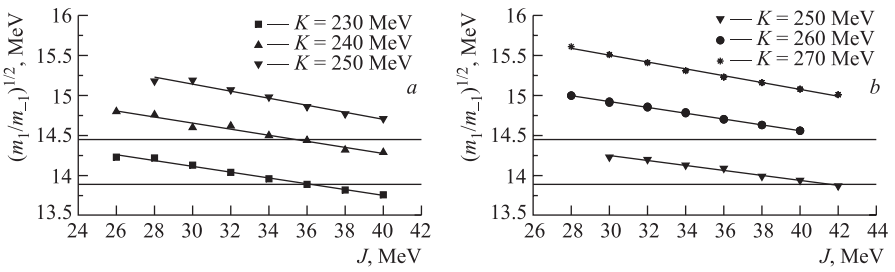

Fig. 5. Constrained ISGMR energies E_{-1} (cf. Eq. (41)) in ^{208}Pb obtained by using the Skyrme forces built in [60], and having $\alpha = 1/6$ (*a*) or $\alpha = 0.3563$ (*b*). The two horizontal lines denote the experimental upper and lower bounds. See the text for a discussion

210 MeV quoted in [1], but to about 235 MeV in clear agreement with the Gogny based extraction of K_∞.

We then discuss the proper comparison between the predictions of the relativistic and the nonrelativistic models. To this aim, parameter sets for Skyrme interactions were generated in [59] by a least-square fitting procedure using the same experimental data for the bulk properties of nuclei considered in [15] for determining the NL3 parameterization of the effective Lagrangian used in the RMF models. Further, the values of the symmetry energy at saturation (J) and the charge r.m.s. radius of the ^{208}Pb nucleus were constrained to be very close to 37.4 MeV and 5.50 fm, respectively, as obtained with the NL3 interaction, and K_∞ was fixed in the vicinity of NL3 value of $K_\infty = 271.76$ MeV. In particular, the Skyrme interactions SK272 and SK255, having $K_\infty = 272$ and 255 MeV, respectively, were generated in [59]. The new Skyrme interaction SK255 yields for the ISGMR centroid energies (E_0) values which are close to the RRPA results obtained for the NL3 interaction, in good agreement with experimental data, despite it has larger K_∞ than other Skyrme sets.

In order to understand this result, a more systematic analysis has been made in [60]. In this work, a larger set of new Skyrme forces has been generated, built with the same protocol used for the Lyon forces [14] and spanning a wide range of values for K_∞, for the symmetry energy at saturation J and its density dependence. The main conclusions reached in that work are the following. The ISGMR energies, calculated by means of CHF, and consequently the extracted value of K_∞, depend on a well-defined parameter ($K_{\rm sym}$), which controls the slope of the symmetry energy curve as a function of density. In fact, it has been shown that there is a correlation between the values of the symmetry energy at saturation J and its slope. The Skyrme forces having a density dependence char-

acterized by an exponent $\alpha = 1/6$, like SLy4, predict K_∞ around 230–240 MeV. If this exponent is increased to values of the order of 1/3, and consequently the slope of the symmetry energy curve is made stiffer, one can produce forces which are compatible with K_∞ around 250–260 MeV. This result, obtained within the framework of a different protocol for fitting the Skyrme parameters, is nonetheless in full agreement with the result of [59]. The main results of [60] are shown in Fig. 5. It has to be noted that a further increase of α, and accordingly of K_∞, would become difficult to obtain since the effective mass m^* would become too small.

One thus can make the clear and strong conclusion that the difference in the values of K_∞ obtained in the relativistic and nonrelativistic models is not due to model dependence. It is mainly due to the different behavior of the symmetry energy within these models (cf. also [61]). One can quote a value of $K_\infty = (240 \pm 20)$ MeV which is somewhat larger than what was previously advocated [1].

7. THE ISGMR IN OTHER MEDIUM-HEAVY NUCLEI

We can better express the idea outlined at the end of the previous section by using Eq. (59) as a guideline. For the sake of simplicity, we rewrite it by neglecting the curvature term and the splitting of the symmetry term into a volume and surface contribution. Two different models (e.g., nonrelativistic and relativistic versions of the mean field) can provide the same value of K_A, so that

$$\begin{aligned} K_A &= K_\infty^{\rm nonrel} + K_{\rm surf}^{\rm nonrel} A^{-1/3} + K_\tau^{\rm nonrel}\delta^2 + K_{\rm Coul}^{\rm nonrel} Z^2 A^{-4/3} + \ldots, \\ K_A &= K_\infty^{\rm rel} + K_{\rm surf}^{\rm rel} A^{-1/3} + K_\tau^{\rm rel}\delta^2 + K_{\rm Coul}^{\rm rel} Z^2 A^{-4/3} + \ldots \end{aligned} \tag{66}$$

The Coulomb contribution does not change much from a nonrelativistic to a relativistic description. However, the surface and symmetry parts (let alone the neglected curvature contribution) could change from one model to the other, so that the extracted K_∞ is also different. This puts in a different perspective the original discussion of [1].

Not so much has been done so far, in order to solve this issue of disentangling the different contributions to the nuclear incompressibility. In [62] it has been claimed that the surface contribution should be approximately proportional to the volume one (similarly to what is known to hold for the corresponding coefficients in the mass formula), but this conclusion is based only on semiclassical calculations.

In order to explore the role of the symmetry term in the above expression, one should abandon the idea of extracting the value of K_∞ from the ISGMR data in a single system, like ^{208}Pb, and consider, for instance, an isotopic chain. The

Sn isotopes are among the longest isotopic chains of spherical nuclei. Therefore, a recent experiment has been performed, using inelastic scattering of α particles at forward angles, at RCNP, Osaka. The results have been reported in [63, 64]. From the cross sections, the strength distributions have been extracted by using the multipole decomposition analysis (cf. Sec. 5). Values of the energies E_0, E_{-1} and E_3 (cf. 3.2) are extracted in the interval 10.5–20.5 MeV and reported here in Table 1.

Table 1. **Ratios of moments of the ISGMR strength distributions (as defined here in 3.2) extracted from the experimental data in [63, 64]. They are evaluated in the energy interval between 10.5 and 20.5 MeV**

Nucleus	E_0	E_{-1}	E_3
^{112}Sn	16.2 ± 0.1	16.1 ± 0.1	16.7 ± 0.2
^{114}Sn	16.1 ± 0.1	15.9 ± 0.1	16.5 ± 0.2
^{116}Sn	15.8 ± 0.1	15.7 ± 0.1	16.3 ± 0.2
^{118}Sn	15.8 ± 0.1	15.6 ± 0.1	16.3 ± 0.1
^{120}Sn	15.7 ± 0.1	15.5 ± 0.1	16.2 ± 0.2
^{122}Sn	15.4 ± 0.1	15.2 ± 0.1	15.9 ± 0.2
^{124}Sn	15.3 ± 0.1	15.1 ± 0.1	15.8 ± 0.1

From the monopole energies reported in the Table a fit of the quantity K_τ has been attempted, by assuming that in Eq. (66) all other terms than the symmetry one are smooth and can be taken as constant along the Sn chain. The fit of

$$K_{\rm A} = a + K_\tau \delta^2, \tag{67}$$

with $\delta = (N-Z)/A$, gives a value $K_\tau = -440 \pm 60$. The main problem emerging here is that the calculations of [60] reproduce the ISGMR energy in ^{208}Pb using interactions characterized by $K_\infty = (230-240)$ MeV and by values K_τ which are well compatible with -440 ± 60; but the same calculations tend to overestimate the experimental ISGMR energies in all the stable even Sn isotopes by almost 1 MeV. Also RMF calculations done along the line of [65] overestimate, although somewhat less, the experimental findings. Another problem is that the results of the Osaka experiment are not compatible with those of [51, 66] performed by the Texas group.

Summarizing, whereas accurate experimental data for the ISGMR in different nuclei are of paramount importance in order to disentangle the different contributions to the nuclear incompressibility, the present availability of results for the stable Sn nuclei does seem, at present, to add problems instead of solving them. Whether this is due to the neglect of the consideration of the surface or curvature contributions, or to pairing or anharmonic effects, it is still not understood.

8. THE ISGDR PROBLEM

The study of the isoscalar giant dipole resonance is very important since this compression mode provides an independent source of information on K_∞. Early experimental investigation of the ISGDR in ^{208}Pb resulted in a value of $E_{\mathrm{ISGDR}} \sim 21$ MeV for the centroid energy [67]. It was first pointed out in [68] that corresponding HF-RPA results for E_{ISGDR}, obtained with interactions adjusted to reproduce experimental values of E_{ISGMR}, are higher than the experimental value by more than 3 MeV and thus this discrepancy between theory and experiment raises some doubts concerning the unambiguous extraction of K_∞ from the energies of compression modes. A similar result for E_{ISGDR} in ^{208}Pb was obtained in more recent experiments [69, 70]. Therefore, the value of K_∞ deduced from these early experimental data on ISGDR is significantly smaller than that deduced from ISGMR data.

It must be stressed that, in contrast with the ISGMR which presents a single peak, as a rule, in heavy nuclei, the dipole response displays a low-lying, fragmented part which lies below the giant resonance. This is a systematic feature of experimental and theoretical results in a number of isotopes. Different theoretical calculations [34, 71] agree in indicating that the low-lying strength is not collective. In fact, while the centroids of the high-energy region, if calculated with interactions associated with different values of K_∞, scale with these values, the centroids of the low-energy region do not. The understanding of the detailed nature of this low-energy component of the ISGDR, represents a great challenge both for experimental and theoretical studies. As far as the giant resonance centroid is concerned, discrete and continuum [72] RPA results are in good agreement with each other in ^{208}Pb. Coupling with $2p-2h$-type configurations is in this case relevant, as it produces a conspicuous spreading width of about 6 MeV [73].

In [36], numerical calculations were carried out for the strength function of the ISGDR, as well as for the cross section $\sigma(E)$ for inelastic α-particle scattering. This latter calculation has been carried out within the single-folding DWBA approach, by employing density-dependent Gaussian α-nucleon interactions, fitted to elastic scattering data. Comparing this microscopically calculated cross section with experimental data should be, in principle, a better procedure than using experimental centroids of the strength distribution. In fact, experimentalists extract strength distributions by assuming collective model transition densities $\delta\rho_{\mathrm{coll}}$ in the whole energy range, whereas we have just discussed that the low-lying strength does not correspond to a collective ISGDR state. In [36] it was found that the shift in the centroid energy, associated with this artificial use of constant, collective $\delta\rho_{\mathrm{coll}}$, is nonetheless small (a few percent) and similar in magnitude to the current experimental uncertainties. On the other hand, it was pointed out that, in the calculation of [36], the maximum cross section for the

ISGDR decreases strongly at high energy and may even drop below the experimental sensitivity for excitation energies above 30 MeV. This high excitation energy region contains about 20% of the EWSR. This missing strength leads to a reduction of about 3.0 MeV in the ISGDR energy which can significantly affect the comparison between theory and experiment. This may be one of the reasons why it is still difficult, in practice, to compare values for K_∞ extracted from the ISGMR and the ISGDR.

Table 2. **Fully self-consistent HF-RPA results [27] for the ISGDR centroid energy (in MeV) in ^{90}Zr and ^{208}Pb, obtained using the interactions SGII and SK255 [59], compared with the RRPA results obtained with the NL3 interaction [15]. Also given are the values of K_∞, and of the symmetry energy at saturation, J. The range of integration is given in the second column**

Nucleus	$E_1 - E_2$	Experiment	NL3	SGII	SK255
^{90}Zr	18–50	25.7 ± 0.7 26.7 ± 0.5 26.9 ± 0.7	32	28.8	29.2
^{208}Pb	16–40	19.9 ± 0.8 22.2 ± 0.5 22.7 ± 0.2	26.0	24.1	24.5
K_∞, MeV			272	215	255
J, MeV			37.4	26.8	37.4

In Table 2 we provide the results of fully self-consistent HF-RPA calculations for the ISGDR centroid energy. The SGII result in ^{208}Pb compares well with 23.9 MeV obtained using discrete RPA in [34] and with 23.4 MeV obtained using continuum RPA in [37]. Note that the HF-RPA values for $E_{\rm ISGDR}$ are larger than the corresponding experimental values of the early measurements of [67, 69, 70] by more than 3 MeV. The more recent results of [51, 52, 74, 75], seem to better agree. Other results of (α,α') inelastic scattering experiments performed on different targets can be found in [76–79].

CONCLUSIONS

The present review paper attempts to give an overview of our present understanding of the compressional modes in finite nuclei, in particular as far as the correlations with basic parameters of the nuclear equation of state (EOS) are concerned. The EOS of symmetric nuclear matter is known to display saturation, that is, there exists a minimum in the energy per particle E/A as a function of the

density ρ. The curvature around this minimum is directly related to the nuclear matter incompressibility K_∞. Only the compressional modes of finite nuclei may shed light on this curvature, in keeping with the fact that a direct determination is not really feasible.

The interest in this quantity is of course not recent. In the seventies and eighties, a first generation of experiments have triggered the first attempts to determine the value of K_∞. The possibility of accelerating isoscalar projectiles like α particles at sufficiently high energy, and of detecting small angle inelastic scattering, has paved the way for a systematic determination of the properties of the ISGMR and ISGDR in many nuclei along the periodic table. Unfortunately, the experimental data alone do not allow a direct extraction of the value of K_∞. In fact, the so-called macroscopic approaches, based on a formula which expresses the finite nucleus incompressibility K_A in terms of volume, surface, symmetry, and Coulomb contributions (like in the mass formula) have been shown to be unreliable and have been soon abandoned. The microscopic way, that is, the idea that the correct value of K_∞ is that associated with a microscopic energy functional which reproduces the monopole energy in finite nuclei, has emerged. The first conclusion from this approach pointed to a value of K_∞ around 220 MeV.

The topic has regained interest in recent years. On the one hand, the experimental techniques allow nowadays a much better determination of the moments of, e.g., the ISGMR strength function. Also the theoretical calculations have been improved and it has been demonstrated that some of the early ones suffer from the lack of full self-consistency. These include some of the calculations which pointed out to the previous value of 220 MeV. More importantly, the concept of a *unique* correlation between the monopole energy in a nucleus and the value of K_∞ has been shown to be not valid. In fact, the relativistic mean field approaches have now become as reliable as the nonrelativistic ones, but within this kind of models larger values of K_∞ are usually extracted, as a rule, than within the nonrelativistic ones.

Recently, some consensus has been reached on few new ideas. First, the nonrelativistic functionals, no matter whether based on Skyrme of Gogny effective forces, point consistently to a value of K_∞ between 230 and 240 MeV. This is somewhat larger than the value which has been proposed so far.

The other important point is that, if the relativistic functionals point to values which are at least around 250 MeV, this is not certainly due to fundamental reasons. It is possible to build Skyrme forces which mimick the same behavior as the relativistic functionals. The compressibility of finite nuclei is of course associated with contributions not only from the volume (this contribution coincides with K_∞) but also from surface, symmetry, etc. Therefore, different classes of functionals may consistently reproduce the ISGMR even if they are associated with different values of K_∞. The relativistic functionals, which successfully

reproduce many nuclear properties having stiffer symmetry energy as compared with the nonrelativistic ones, point to values of K_∞ around 250–270 MeV.

One can conclude that the remaining uncertainty on K_∞, which we would set at present in the range (240 ± 20) MeV, is mainly related to the lack of understanding of the global features of the functionals, mainly of their density dependence. Softer (stiffer) symmetry energies are, e.g., associated with less (more) negative values of the symmetry contribution to the finite nucleus compressibility and, consequently, to smaller (larger) values of K_∞.

This conclusion has mainly been reached by studying the ISGMR in ^{208}Pb. Other nuclei, like the Sn isotopes, which have been analyzed with the hope of clarifying this issue, have indeed caused more trouble. The different contributions to the compressibility should be carefully reexamined in order to have better insight into this longstanding problem. Last but not least, we still lack a unified picture from the ISGMR and the ISGDR. The main problem has been, so far, the presence of noncollective and noncompressional isoscalar dipole stength. Probably, independent progresses concerning our general understanding of the nuclear energy functionals may provide new insight into these problems.

Acknowledgements. The author would like to acknowledge the enormous benefit from either discussions or collaboration with K. Bennaceur, P. Bonche, P. F. Bortignon, M. Centelles, S. Fracasso, U. Garg, I. Hamamoto, Y.-W. Lui, J. Meyer, Nguyen Van Giai, J. Piekarewicz, M. R. Quaglia, P. Ring, H. Sagawa, M. Uchida, D. Vretenar, and D. H. Youngblood.

REFERENCES

1. *Blaizot J. P.* Nuclear Compressibilities // Phys. Rep. 1980. V. 64. P. 171–248.
2. *Colò G., Van Giai N.* Theoretical Understanding of the Nuclear Incompressibility: Where Do We Stand? // Collective Motion in Nuclei under Extreme Conditions (COMEX1). Paris, 2003; Nucl. Phys. A. 2004. V. 731. P. 15–27.
3. *Colò G., Van Giai N.* Relativistic and Nonrelativistic Calculations of the Isoscalar Monopole and Dipole States // Intern. Conf. on Nuclear Structure and Related Topics (NRST2003); Phys. At. Nucl. 2004. V. 67. P. 1759–1763.
4. *Shlomo S., Kolomietz V.M., Colò G.* Deducing the Nuclear-Matter Incompressibilty Coefficient from Data on Isoscalar Compression Modes // Eur. Phys. J. A. 2006. V. 30. P. 23–30.
5. *Paar N. et al.* Exotic Modes of Excitation in Atomic Nuclei Far from Stability // Rep. Progr. Phys. 2007. V. 70. P. 691–793.
6. *Skyrme T. H. R.* The Effective Nuclear Potential // Nucl. Phys. 1959. V. 9. P. 615–634.
7. *Vautherin D., Brink D. M.* Hartree–Fock Calculations with Skyrme's Interaction: I. Spherical Nuclei // Phys. Rev. C. 1972. V. 5. P. 626–647.

8. *Beiner M. et al.* Nuclear Ground-State Properties and Self-Consistent Calculations with the Skyrme Interaction: I. Spherical Description // Nucl. Phys. A. 1975. V. 238. P. 29–69.

9. *Bender M., Heenen P.-H., Reinhard P.-G.* Self-Consistent Mean-Field Models for Nuclear Structure // Rev. Mod. Phys. 2003. V. 75. P. 121–180.

10. *Dechargé J., Gogny D.* Hartree–Fock–Bogolyubov Calculations with the $D1$ Effective Interaction on Spherical Nuclei // Phys. Rev. C. 1980. V. 21. P. 1568–1593.

11. *Berger J. F., Girod M., Gogny D.* Time-Dependent Quantum Collective Dynamics Applied to Nuclear Fission // Comp. Phys. Commum. 1991. V. 63. P. 365–374.

12. *Ring P., Schuck P.* The Nuclear Many-Body Problem. Springer-Verlag, 1980. 717 p.

13. *Brown B. A.* Neutron Radii in Nuclei and the Neutron Equation of State // Phys. Rev. Lett. 2000. V. 85. P. 5296–5298;
Furnstahl R. J. Neutron Radii in Mean-Field Models // Nucl. Phys. A. 2002. V. 706. P. 85–110;
Steiner A. W. et al. Isospin Asymmetry in Nuclei and Neutron Stars // Phys. Rep. 2005. V. 411. P. 325–375.

14. *Chabanat E. et al.* A Skyrme Parametrization from Subnuclear to Neutron Star Densities // Nucl. Phys. A. 1998. V. 635. P. 231–256.

15. *Lalazissis G. A., König J., Ring P.* New Parametrization for the Lagrangian Density of Relativistic Mean Field Theory // Phys. Rev. C. 1997. V. 55. P. 540–543.

16. *Serot B. D., Walecka J. D.* The Relativistic Nuclear Many-Body Problem // Adv. Nucl. Phys. 1986. V. 16. P. 1–327.

17. *Vretenar D. et al.* Relativistic Hartree–Bogoliubov Theory: Static and Dynamic Aspects of Exotic Nuclear Structure // Phys. Rep. 2005. V. 409. P. 101–259.

18. *Bürvenich T. et al.* Nuclear Ground State Observables and QCD Scaling in a Refined Relativistic Point Coupling Model // Phys. Rev. C. 2002. V. 65. P. 044308-1–044308-23.

19. *Long W. H. et al.* Pseudo-Spin Symmetry in Density Dependent Relativistic Hartree–Fock Theory // Phys. Lett. B. 2006. V. 639. P. 242–247.

20. *Rowe D. J.* Nuclear Collective Motion. Methuen, 1970. 340 p.

21. *Bertsch G. F., Tsai S. F.* A Study of the Nuclear Response Function // Phys. Rep. 1975. V. 18. P. 125–158.

22. *Bohigas O., Lane A. M., Martorell J.* Sum Rules for Nuclear Collective Excitations // Phys. Rep. 1979. V. 52. P. 267–316.

23. *Agrawal B. K., Shlomo S., Sanzhur A. I.* Self-Consistent Hartree–Fock Based Random Phase Approximation and the Spurious State Mixing // Phys. Rev. C. 2003. V. 67. P. 034314-1–034314-14;
Agrawal B. K., Shlomo S. Consequences of Self-Consistency Violations in Hartree–Fock Random-Phase Approximation Calculations of the Nuclear Breathing Mode Energy // Phys. Rev. C. 2004. V. 70. P. 014308-1–014308-4.

24. *Terasaki J. et al.* Self-Consistent Description of Multipole Strength in Exotic Nuclei: Method // Phys. Rev. C. 2005. V. 71. P. 034310-1–034310-15.

25. *Peru S., Berger J. F., Bortignon P. F.* Giant Resonances in Exotic Spherical Nuclei within the RPA Approach with the Gogny Force // Eur. Phys. J. A. 2005. V. 26. P. 25–32.

26. *Fracasso S., Colò G.* The Fully Self-Consistent Charge-Exchange QRPA and Its Application to the Isobaric Analog Resonances // Phys. Rev. C. 2005. V. 72. P. 064310-1–064310-9.

27. *Sil T. et al.* Effects of Self-Consistency Violation in Hartree–Fock RPA Calculations for the Nuclear Giant Resonances Revisited // Phys. Rev. C. 2006. V. 73. P. 034316-1–034316-7.

28. *Colò G. et al.* What Can We Learn from Recent Nonrelativistic Mean Field Calculations? // Nucl. Phys. A. 2007 (in press).

29. *Van Giai N., Sagawa H.* Spin-Isospin and Pairing Properties of Modified Skyrme Interactions // Phys. Lett. B. 1981. V. 106. P. 379–382.

30. *Lipparini E., Stringari S.* Sum Rules and Giant Resonances in Nuclei // Phys. Rep. 1989. V. 175. P. 103–261.

31. *Lane A. M., Martorell J.* The Random Phase Approximation: Its Role in Restoring Symmetries Lacking in the Hartree–Fock Approximation // Ann. Phys. (N. Y.). 1980. V. 129. P. 273–302.

32. *Blaizot J. P., Ripka G.* Quantum Theory of Finite Systems. The MIT Press, 1986. 657 p.

33. *Bertsch G.F.* The Nuclear Response Function // Progr. Theor. Phys. Suppl. 1983. V. 74–75. P. 115–141.

34. *Colò G. et al.* On Dipole Compression Modes in Nuclei // Phys. Lett. B. 2000. V. 485. P. 362–366.

35. *Van Giai N., Sagawa H.* Monopole and Dipole Compression Modes in Nuclei // Nucl. Phys. A. 1981. V. 371. P. 1–18.

36. *Kolomiets A., Pochivalov O., Shlomo S.* Microscopic Description of Excitation of Nuclear Isoscalar Giant Resonances by Inelastic Scattering of 240 MeV α Particles // Phys. Rev. C. 2000. V. 61. P. 034312-1–034312-8;
Shlomo S., Sanzhur A. I. Isoscalar Giant Dipole Resonance and Nuclear Matter Incompressibility Coefficient // Phys. Rev. C. 2002. V. 65. P. 044310-1–044310-5.

37. *Hamamoto I., Sagawa H.* Isoscalar Dipole Strength in $^{208}_{82}\mathrm{Pb}_{126}$: The Spurious Mode and the Strength in the Continuum // Phys. Rev. C. 2002. V. 66. P. 044315-1–044315-7.

38. *Glendenning N.K.* Equation of State from Nuclear and Astrophysical Evidence // Phys. Rev. C. 1988. V. 37. P. 2733–2743.

39. *Myers W. D., Swiatecki W. J.* Nuclear Equation of State // Phys. Rev. C. 1998. V. 57. P. 3020–3025.

40. *Satpathy L., Uma Maheswari V. S., Nayak R. C.* From Nuclei to Nuclear Matter: A Leptodermous Approach // Phys. Rep. 1999. V. 319. P. 85–144.

41. *Blaizot J. P. et al.* Microscopic and Macroscopic Determination of Nuclear Compressibility // Nucl. Phys. A. 1995. V. 591. P. 435–457.

42. *Von Oertzen W., Bohlen H. G., Khoa D. T.* Nuclear Rainbow and the EOS of Nuclear Matter // Nucl. Phys. A. 2003. V. 722. P. 202–208.

43. *Khoa D. T. et al.* Nuclear Rainbow Scattering and Nucleus–Nucleus Potential // J. Phys. G: Nucl. Part. Phys. 2007. V. 34. P. R111–R164.

44. *Natowitz J. B. et al.* Limiting Temperatures and the Equation of State of Nuclear Matter // Phys. Rev. Lett. 2002. V. 89. P. 212701-1–212701-4.

45. *Shlomo S., Youngblood D. H.* Nuclear Matter Compressibility from Isoscalar Giant Monopole Resonance // Phys. Rev. C. 1993. V. 47. P. 529–536.

46. *Pearson J. M.* The Incompressibility of Nuclear Matter and the Breathing Mode // Phys. Lett. B. 1991. V. 271. P. 12–16.

47. *Treiner J. et al.* Nuclear Incompressibility: From Finite Nuclei to Nuclear Matter // Nucl. Phys. A. 1981. V. 371. P. 253–287.

48. *Van Giai N. et al.* Compression Modes in Nuclei: Theoretical Approaches // Intern. Conf. on Giant Resonances. Osaka, 2000; Nucl. Phys. A. 2001. V. 687. P. 44–51.

49. *Colò G., Bortignon P. F., Van Giai N., Bracco A., Broglia R. A.* Damping Properties of the Breathing Mode in ^{208}Pb // Phys. Lett. B. 1992. V. 276. P. 279–284.

50. *Bertsch G. F., Bortignon P. F., Broglia R. A.* Damping of Nuclear Excitations // Rev. Mod. Phys. 1983. V. 55. P. 287–314.

51. *Youngblood D. H. et al.* Isoscalar $E0 - E3$ Strength in ^{116}Sn, ^{144}Sm and ^{208}Pb // Phys. Rev. C. 2004. V. 69. P. 034315-1–034315-14.

52. *Youngblood D. H., Clark H. L., Lui Y. W.* Compression Mode Resonances in ^{90}Zr // Phys. Rev. C. 2004. V. 69. P. 054312-1–054312-6.

53. *Satchler G. R.* Direct Nuclear Reactions. Oxford Univ. Press, 1983. 833 p.

54. *Satchler G. R., Khoa D. T.* Missing Monopole Strength in ^{58}Ni and Uncertainties in the Analysis of α-Particle Scattering // Phys. Rev. C. 1997. V. 55. P. 285–297.

55. *Ma Z. et al.* Isoscalar Compression Modes in Relativistic Random Phase Approximation // Nucl. Phys. A. 2001. V. 686. P. 173–186.

56. *Vretenar D., Nikšič T., Ring P.* A Microscopic Estimate of the Nuclear Matter Compressibility and Symmetry Energy in Relativistic Mean-Field Models // Phys. Rev. C. 2003. V. 68. P. 024310-1–024310-9.

57. *Hamamoto I., Sagawa H., Zhang X. Z.* Giant Monopole Resonances in Nuclei near Stable and Drip Lines // Phys. Rev. C. 1997. V. 56. P. 3121–3133.

58. *Colò G. et al.* Compression Modes in Nuclei: RPA and QRPA Predictions with Skyrme Interactions // Intern. Conf. on Nuclear Structure and Related Topics (NRST2000), Dubna, 2000; Yad. Fiz. 2001. V. 64. P. 1119–1122.

59. *Agrawal B. K., Shlomo S., Au V. K.* Nuclear Matter Incompressibility Coefficient in Relativistic and Nonrelativistic Microscopic Models // Phys. Rev. C. 2003. V. 68. P. 031304-1–031304-5;
Shlomo S., Agrawal B. K., Au V. K. Status of the Nuclear Matter Equation of State as Determined from Compression Modes // Nucl. Phys. A. 2004. V. 734. P. 589–592.

60. *Colò G. et al.* Microscopic Determination of the Nuclear Incompressibility within the Nonrelativistic Framework // Phys. Rev. C. 2004. V. 70. P. 024307-1–024307-9.

61. *Piekarewicz J.* Correlating the Giant-Monopole Resonance to the Nuclear-Matter Incompressibility // Phys. Rev. C. 2002. V. 66. P. 034305-1–034305-5.

62. *Patra S. K. et al.* Surface Incompressibility from Semiclassical Relativistic Mean Field Calculations // Phys. Rev. C. 2002. V. 65. P. 044304-1–044304-7.

63. *Garg U.* The Giant Monopole Resonance in the Sn Isotopes: Why Is Tin So «Fluffy»? // Nucl. Phys. A. 2007 (in press).

64. *Li T. et al.* Isotopic Dependence of the Giant Monopole Resonance in the Even-A $^{112-124}$Sn Isotopes and the Asymmetry Term in Nuclear Incompressibility. To be published.

65. *Todd-Rutel B. G., Piekarewicz J.* Neutron-Rich Nuclei and Neutron Stars: A New Accurately Calibrated Interaction for the Study of Neutron-Rich Matter // Phys. Rev. Lett. 2005. V. 95. P. 122501-1–122501-4.

66. *Lui Y.-W. et al.* Giant Resonances in ^{112}Sn and ^{124}Sn: Isotopic Dependence of Monopole Resonance Energies // Phys. Rev. C. 2004. V. 70. P. 014307-1–014307-7.

67. *Morsch H. P. et al.* New Giant Resonances in 172-MeV α Scattering from ^{208}Pb // Phys. Rev. Lett. 1980. V. 45. P. 337–340;
Djalali D. et al. 201 MeV Proton Excitation of Giant Resonances in ^{208}Pb: Macroscopic and Microscopic Analysis // Nucl. Phys. A. 1982. V. 380. P. 42–60.

68. *Dumitrescu T. S., Serr F. E.* Self-Consistent Calculations of Dipole and Quadrupole Compression Modes // Phys. Rev. C. 1983. V. 27. P. 811–815.

69. *Clark H. L., Lui Y. W., Youngblood D. H.* Isoscalar Giant Dipole Resonance in ^{90}Zr, ^{116}Sn and ^{208}Pb // Phys. Rev. C. 2001. V. 63. P. 031301(R)-1–031301(R)5.

70. *Davis B. F. et al.* Evidence for the Isoscalar Giant Dipole Resonance in ^{208}Pb Using Inelastic α Scattering at and near 0° // Phys. Rev. Lett. 1997. V. 79. P. 609–612.

71. *Vretenar D., Wandelt A., Ring P.* Isoscalar Dipole Mode in Relativistic Random Phase Approximation // Phys. Lett. B. 2000. V. 487. P. 334–340.

72. *Hamamoto I., Sagawa H., Zhang X. Z.* Isoscalar and Isovector Dipole Mode in Drip Line Nuclei in Comparison with β-Stable Nuclei // Phys. Rev. C. 1998. V. 57. P. R1064–R1068.

73. *Colò G. et al.* Compression Modes in Nuclei: Microscopic Models with Skyrme Interactions // RIKEN Symp. on Selected Topics in Nuclear Collective Excitations. RIKEN, 1999; RIKEN Rev. 1999. V. 23. P. 39–42.

74. *Uchida M. et al.* Systematics of the Bimodal Isoscalar Giant Dipole Resonance // Phys. Rev. C. 2004. V. 69. P. 051301(R)-1–051301(R)5.

75. *Itoh M. et al.* Systematics Study of $L = 0 - 3$ Giant Resonances in Sm Isotopes via Multipole Decomposition Analysis // Phys. Rev. C. 2003. V. 68. P. 064602-1–064602-10.

76. *Clark H. L. et al.* Isoscalar Giant Dipole Resonance in ^{90}Zr, ^{116}Sn, ^{144}Sm, and ^{208}Pb Excited by 240 MeV α-Particle Scattering // Nucl. Phys. A. 1999. V. 649. P. 57c–60c.

77. *Clark H. L., Lui Y. W., Youngblood D. W.* Isoscalar Giant Dipole Resonance in ^{90}Zr, ^{116}Sn, and ^{208}Pb // Phys. Rev. C. 2001. V. 63. P. 031301(R)-1–031301(R)-5.

78. *Uchida M. et al.* Isoscalar Giant Dipole Resonance in ^{208}Pb via Inelastic α Scattering at 400 MeV and Nuclear Incompressibility // Phys. Lett. B. 2003. V. 557. P. 12–19.

79. *Garg U.* The Isoscalar Giant Resonance: A Status Report // Nucl. Phys. A. 2004. V. 731. P. 3–14.